We are IntechOpen,
the world's leading publisher of
Open Access books
Built by scientists, for scientists

6,900
Open access books available

186,000
International authors and editors

200M
Downloads

Our authors are among the

154
Countries delivered to

TOP 1%
most cited scientists

12.2%
Contributors from top 500 universities

CLARIVATE ANALYTICS
BOOK CITATION INDEX
INDEXED

WEB OF SCIENCE™

Selection of our books indexed in the Book Citation Index
in Web of Science™ Core Collection (BKCI)

Interested in publishing with us?
Contact book.department@intechopen.com

Numbers displayed above are based on latest data collected.
For more information visit www.intechopen.com

Ultrastructure of Dentogingival Border of Normal and Replanted Tooth and Dental Implant

Takashi Sawada[1] and Sadayuki Inoue[2]
[1]Department of Ultrastructural Science, Tokyo Dental College,
[2]Department of Anatomy and Cell Biology, McGill University,
[1]Japan
[2]Canada

1. Introduction

The interface between the gingiva and the tooth enamel is characterized by the presence of an attachment apparatus composed of well-developed hemidesmosomes at the basal surface of the junctional epithelium and internal basement membrane (Schroeder, 1986; Bosshardt & Lang, 2005). This apparatus plays an important role in the firm attachment of the epithelium to the tooth and in sealing the periodontal tissue from the oral environment. High resolution ultrastructural studies in our laboratory provided further evidence of this effective sealing (Sawada & Inoue, 1996, 2001a, 2003). In the first part of this review article, the ultrastructure of the dentogingival border in a normal tooth is described in detail.

The original attachment apparatus is mechanically broken down immediately after any surgical procedure such as tooth replantation or implantation. Whether the attachment apparatus is regenerated at the dento (implant)-gingival border in either case remains to be determined. In the latter half of this article, we will, therefore, describe the ultrastructure of the dentogingival border in replanted teeth and implants based upon our recent study (Shioya et al., 2009).

2. Materials and methods

The animals used in this study were as follows: Japanese monkeys (*Macaca fuscata*) and Rhesus monkeys (*Macaca mulatta*) provided by the Primate Research Institute of Kyoto University, Kyoto, Japan; a shark (*Cephaloscyllium umbratile*) freshly caught off the coast of Suruga, Shizuoka Prefecture, Japan; and Wistar rats purchased from CLEA JAPAN, Inc., Tokyo, Japan. All experiments were performed in accordance with the "Guidelines for the Use of Experimental Animals at Tokyo Dental College".

2.1 Monkeys

The head and neck regions of 3-5-year-old monkeys were perfused, under anesthesia, with a fixative containing 2.5% glutaraldehyde and 2% formaldehyde in 0.1M sodium cacodylate buffer, pH 7.4, through the carotid arteries for 60 min. Isolated upper and lower jaws were

further fixed by immersing them in the same fresh fixative for 24 hr at 4°C. Molars with associated gingiva were isolated and washed with 0.1 M sodium cacodylate buffer containing 0.2 M sucrose. An aliquot of teeth was demineralized in 10% EDTA for 6-8 weeks at 4°C. Both demineralized and non-demineralized tissues were postfixed with 1% osmium tetroxide in 0.1 M sodium cacodylate buffer for 1.5 hr at 4°C, dehydrated in a graded series of ethanol, and embedded in epoxy resin. Semi-thin sections were stained with toluidine blue for light microscopy. Thin sections of tissue containing the internal basement membrane spanning from the cemento-enamel junction to the gingival groove were prepared for observation with either the H-7100 or H-7650 electron microscope (Hitachi Co., Tokyo, Japan), with or without counterstaining with uranyl acetate and lead citrate, and operating at 100 kV.

2.2 Shark

Tooth-bearing jaws of a shark were dissected out under anesthesia with MS222 and cut into small pieces. The pieces were fixed by placing them in a fixative containing 2.5% glutaraldehyde and 2% formaldehyde in 0.1 M sodium phosphate buffer, pH 7.4, for 24 hr at 4°C. An aliquot of the specimens was demineralized in 10% EDTA for 3-4 weeks at 4°C. Both demineralized and non-demineralized tissues were postfixed with 1% osmium tetroxide in 0.1 M sodium phosphate buffer for 1.5 hr at 4°C. They were further processed as described above for the observation of semi-thin and thin sections.

2.3 Rats

Experiment I: Tooth replantation was performed by a previously described method (Ihara et al., 2007). Briefly, under general anesthesia with ketamine hydrochloride, upper right molars were luxated with a dental excavator and carefully extracted with forceps in order to avoid damaging surrounding tissues. Then, they were immediately replaced in their original sockets. Gingiva around the maxillary left first molars was used as a control. All animals were allowed free access to water and a powdered diet. For ultrastructural examination as described below, the animals were sacrificed at 1, 2 or 4 weeks after the procedure.

Experiment II: After extraction of the tooth by the method described above, a screw-type implant was immediately placed in the socket. A custom-made pure titanium implant (Ti) (Fig. 1) 1.6 mm in diameter and 4 mm in length was used (Platon Japan Co., Tokyo, Japan). Sufficient space was left between the opposing lower first molar and the implant to avoid occlusal stimuli during mastication. After the operation, the animals were allowed access to water and a powdered diet *ad libitum*. They were sacrificed in groups at 1, 2, 4 or 8 weeks after the operation.

Under anesthesia with ketamine hydrochloride, the animals were perfused with a cold fixative containing 2.5% glutaraldehyde and 2% formaldehyde in 0.1 M sodium phosphate buffer, pH 7.4, for 20 min. Isolated upper jaws were further fixed by immersing them in the same fresh fixative for 5 hr at 4°C, after which they were washed with sodium phosphate buffer and demineralized in 10% EDTA for 4 weeks at 4°C. In experiment II, implants were mechanically separated from the surrounding tissue according to the method of Ikeda et al. (2000). Both replanted teeth with gingiva and peri-implant tissues were postfixed with 1% osmium tetroxide in 0.1 M sodium phosphate buffer for 1 hr, dehydrated in a graded series of ethanol, and embedded in epoxy resin. Thin sections were stained with uranyl acetate and lead citrate before observation by electron microscopy.

Fig. 1. Photograph showing rat upper jaw implanted with custom-made pure titanium implant

3. Ultrastructure of dentogingival border

3.1 Attachment apparatus in normal tooth

The surface (enamel) of the tooth is known to attach to the gingiva by means of an attachment apparatus. This attachment apparatus is composed of the hemidesmosomes of the junctional epithelium and the internal basement membrane (Listgarten, 1966, 1972; Schroeder, 1969; Schroeder & Listgarten, 1977; Stern, 1981). The internal basement membrane was initially described as an 80-120-nm wide homogeneous layer (Stern, 1981). It directly faced the enamel, and an intervening laminated or non-laminated layer of cuticles was found to be present in dog (Matsson et al., 1979), pig (Marks et al., 1994), monkey (Kobayashi et al., 1976; Sawada & Inoue, 2001b) and man (Listgarten, 1966; Schroeder & Listgarten, 1977). The internal basement membrane was either directly facing the surface of the enamel or doing so through intervening layers of cuticles (Kobayashi et al., 1976; Sawada & Inoue, 2001b) or afibrillar cementum in rhesus monkey (Kobayashi et al., 1976). The latter authors also reported that numerous fine strands crossed the lamina densa of the internal basement membrane at the hemidesmosomes. These strands may have been the anchoring filaments of hemidesmosomes, reported to be composed of kalinin and epiligrin (Eady, 1994; Garrod, 1993). In the cytoplasm of the cells of the junctional epithelium, the tonofibrils are associated with hemidesmosomes.

A more recent study investigated the internal basement membrane of the dentogingival border in monkey by transmission electron microscopy (Fig. 2) and found that it was uniquely specialized for mechanical strength, sealing off the periodontal tissues from the oral environment (Sawada & Inoue, 1996). Morphologically, basement membranes may be classified into three types: common, "thin" basement membranes; "double" basement membranes such as glomerular basement membrane; and often multilayered, "thick" basement membranes such as Reichert's membrane, the lens capsule, and the basement membrane matrix of mouse EHS tumor (Inoue, 1989).
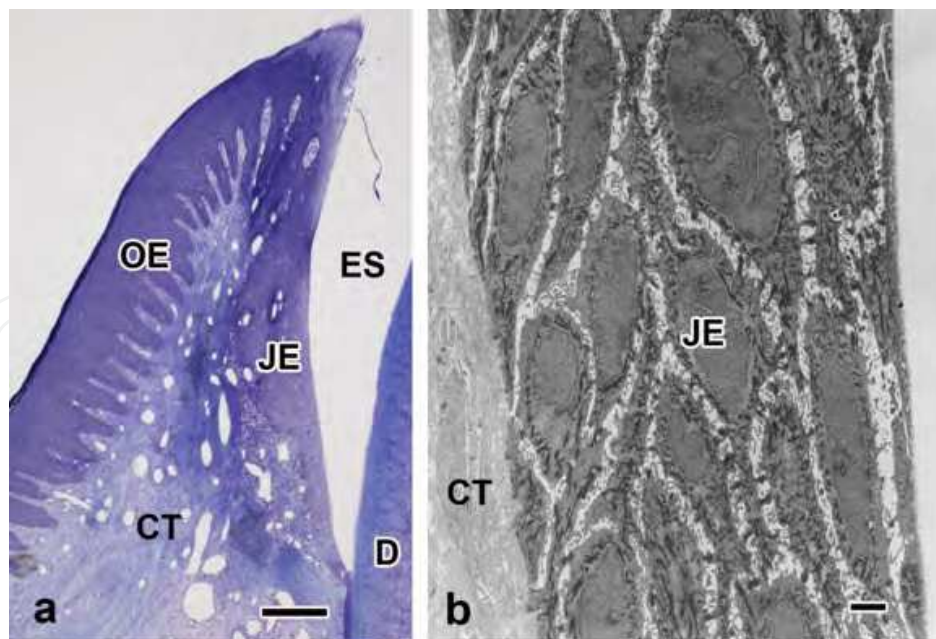
Junctional epithelium (JE) is bordered by enamel (enamel space, ES) and supporting gingival connective tissue (CT). OE, oral epithelium; D, dentin. Scale bars = 100 μm (a), 2 μm (b). Modified from Sawada & Inoue, 2003 © Calcified Tissue International.

Fig. 2. Light micrograph (a) of semi-thin section and electron micrograph (b) of thin section of an area of dentogingival border of monkey tooth

Firstly, in monkey, the internal basement membrane is unique in that it takes the form of both thin and multilayered thick basement membranes (Fig. 3). The thickening and multi-layering of the basement membrane may be directly related to the role of specific basement membranes such as the multilayered Reichert's membrane of the parietal yolk sac (Inoué et al., 1983). The capsular portion of Reichert's membrane provides reinforcement to the parietal wall of the embryonic yolk sac (Jollie, 1968). Similarly, multilayered internal basement membrane may provide mechanical strength for firm attachment of the tooth to the gingiva and the sealing off of the periodontal tissues from the oral environment. The monolayered, thin basement membrane portion of the internal basement membrane is also unique. This lamina densa, at 160 nm in width, is unusually thick compared with 30-80 nm in other types of basement membrane. Another example of unusually thick basement membrane is that of seminiferous tubules in rat (Inoue & Leblond, 1988). Again, the role of this particular basement membrane is mechanical strength to protect the integrity of the epithelium against the rhythmic contractions of the seminiferous tubules for the movement of sperm. Similarly, unusual thickening of the monolayered part of the internal basement membrane at the dentogingival border may provide mechanical strength for the tight sealing of this border.

Secondly, the finer level structure of the internal basement membrane, that is, the "cord" network, is also unique (Fig. 4). In basement membrane, in general, the basic texture of the lamina densa is made up of a 3-dimensional network formed by anastomosing, irregular, thread-like structures referred to as "cords" (Inoue, 1989, 1994; Sawada & Inoue, 2001a). In most types of basement membrane, the thickness of the cord is 3 nm-5 nm, and the average size of the openings in the network ("intercordal space diameter index") is 14 nm. The average thickness of the cords and the size of the openings in the internal basement

membrane are 8.3 nm and 18.9 nm, respectively (Sawada & Inoue, 1996). These unusually wide cords and large openings are similar to those found in Reichert's membrane (5 nm and 15 nm, respectively) and the basement membrane of seminiferous tubules (4.5 nm and 14.1 nm, respectively). This indicates the role of the cord network in the mechanical strength of the internal basement membrane.
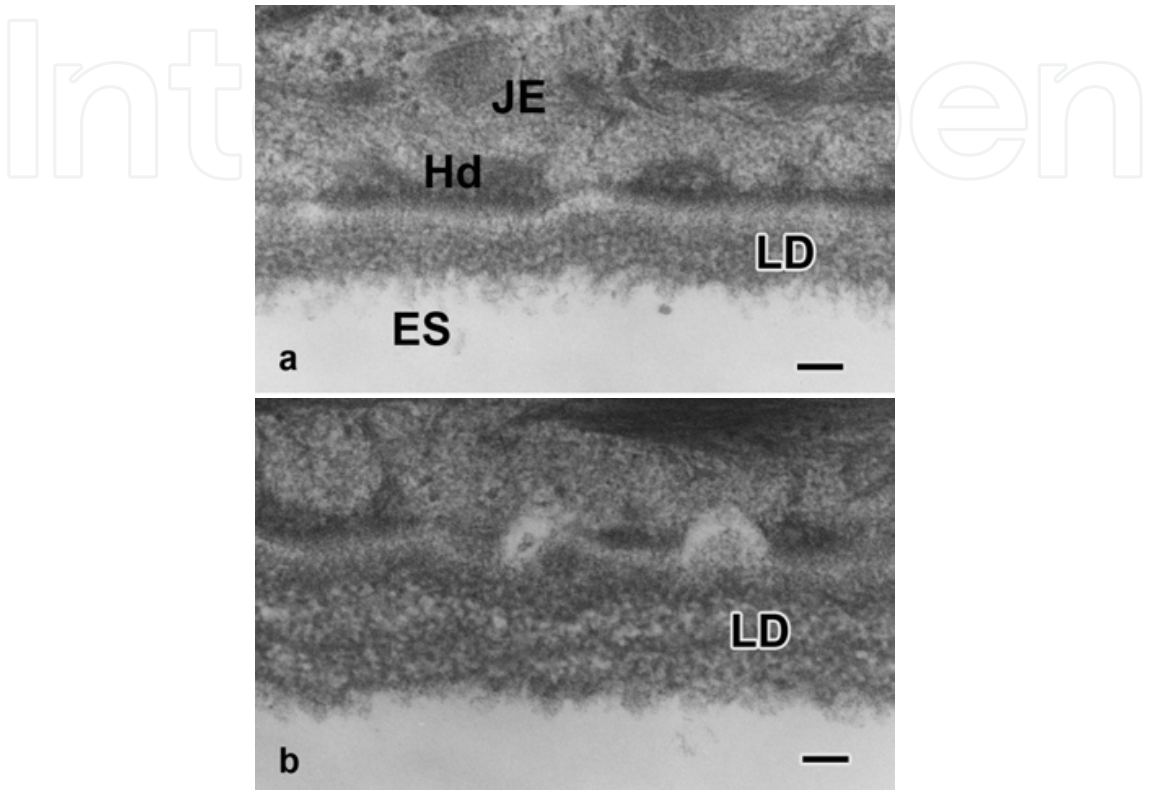
Internal basement membrane is composed of either single broad lamina densa (a) or multi-layers (b). JE, junctional epithelium; LD, lamina densa; Hd, hemidesmosomes; ES, enamel space. Scale bars = 0.1 μm. Modified from Sawada & Inoue, 1996 © The Anatomical Record.

Fig. 3. Electron micrograph of internal basement membrane of junctional epithelium
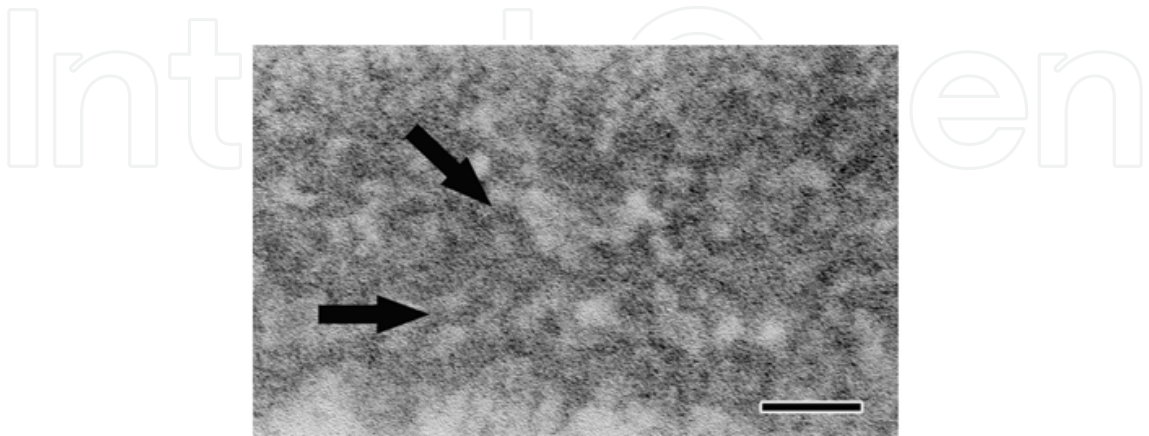
Lamina densa is composed of fine network of irregular anastomosing cords (indicated by arrows). Scale bar = 50 nm. Modified from Sawada & Inoue, 1996 © The Anatomical Record.

Fig. 4. High-magnification view of internal basement membrane of monkey tooth

3.2 Dental cuticle at dentogingival border

The dental cuticle is usually found at the dentogingival border in healthy teeth or at the surface of the roots of teeth with periodontal disease. Ultrastructurally, the dental cuticle has been described as an electron-dense, non-mineralized organic structure with an unlaminated amorphous appearance (Schroeder, 1986). In adult periodontitis, the dental cuticle covering the cementum showed a lobulated and layered structure with perforations (Friedman et al., 1993). Histochemical studies indicated that the structure may contain a protein-rich material (Kobayashi & Rose, 1978, 1979; López et al., 1990), or anionic polymers including glycoproteins (Friedman et al., 1993). Based on the results of morphological, as well as histochemical studies, the origin of the dental cuticle has been suggested to be a secretory product of the junctional epithelium (Ito et al., 1967; Listgarten, 1970; Nagatsuka, 1983; Sato, 1973; Schroeder & Listgarten, 1971), that is, either the accumulation of basement membrane components produced by the cells of the epithelium, or the formation of a layer of serum proteins originating from gingival exudates in the process of aging (Eide et al., 1983; Frank & Cimasoni, 1970; Friedman et al., 1993; Lie & Selvig, 1975; López et al., 1990); it has also been suggested to originate in hemoglobin resulting from the degradation of red blood cells (Hodson, 1966). Thus, its origin has yet to be conclusively determined.

In our previous study (Sawada & Inoue, 2001b), the detailed ultrastructural nature of the dental cuticle in monkey tooth was examined by high resolution electron microscopy. The dental cuticle, seen as a dense amorphous, usually unlaminated layer, was localized between the internal basement membrane and the enamel surface (Fig. 5a). High resolution electron microscopy showed that its basic structure was a fine network of irregular anastomosing strands identified as the cord network of the basement membrane of the junctional epithelium, as described above (Fig. 5b).

In the cuticle, openings of most of the network were filled with a dark amorphous material. Based upon the data, it was suggested that an additional layer of cord network formed from basement membrane components probably secreted by cells of the junctional epithelium during formation of the cuticle is added to the cord network of the lamina densa of the basement membrane. In addition, a dark amorphous material is deposited within the newly added cord network at the enamel side of the basement membrane. The origin of this dark material still remains to be clarified, but it possibly originates, as has previously been suggested, from either serum protein in gingival exudates or from hemoglobin produced by the degradation of red blood cells.

3.3 Mechanism of binding of normal tooth to gingiva

Detailed ultrastructural observation of the dentogingival border was carried out to elucidate how comparatively strong binding of the tooth to the gingiva is achieved in mammals (monkey) and non-mammalian vertebrates (shark) (Sawada & Inoue, 2003).

In monkey, this specialization of the lamina densa of the internal basement membrane is closely associated with an additional layer referred to as the supplementary lamina densa found on the enamel side of the tooth (Fig. 6a). Observation of non-demineralized tissue revealed that one part of the basement membrane, the supplementary lamina densa, was mineralized (Fig. 6b). This mineral deposit was continuous with that of the enamel of the tooth, and thus this deposit on the supplementary lamina densa formed an advancing edge of mineralization. Under this arrangement, two different phases, an organic and a mineral phase, overlap, with direct contact at this part of the basement membrane, ensuring intimate

contact between and strong binding of these phases. Furthermore, detailed observation revealed that, in the mineralized portion of the lamina densa, mineral crystals were arranged in a network pattern which was comparable to the pattern of the cord network. This may facilitate more powerful gripping, and further demonstrates the elaborate mechanism by which firm binding of the mineral and organic phases is achieved.
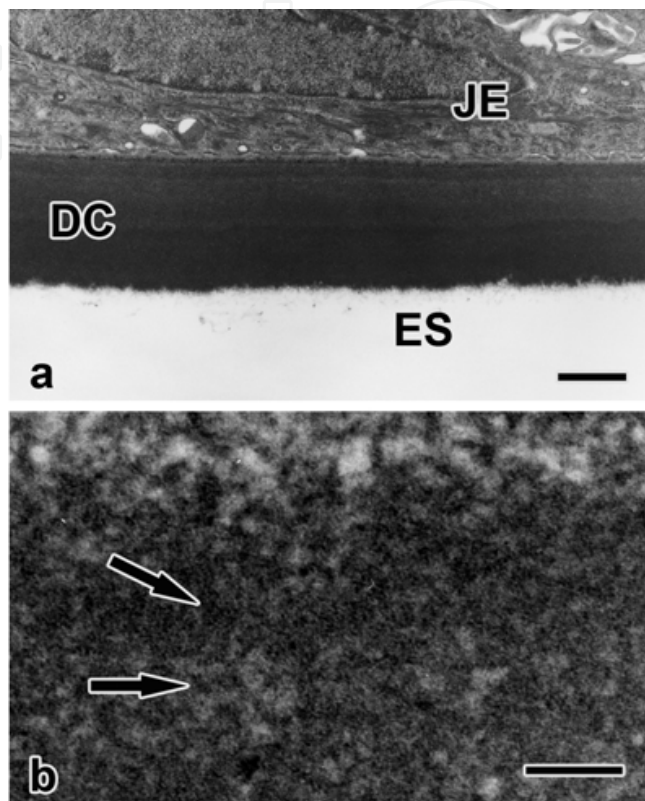
Cuticle contains network anastomosing structure (arrows) resembling cord network of internal basement membrane. Intercordal space is filled with dark amorphous material. JE, junctional epithelium; ES, enamel space. Scale bars = 1 μm (a), 0.1 μm (b). Modified from Sawada & Inoue, 2001b © Journal of Periodontal Research.

Fig. 5. (a) Dental cuticle (DC) found at dentogingival border in monkey (b) High magnification view of dental cuticle

The specialization of the lamina densa of the internal basement membrane in shark tooth was more complex (Fig. 7). Along the surface of the lamina densa of the internal basement membrane facing the oral epithelium (junctional epithelium), hemidesmosome-related, semicircular or rectangular bulges were intermittently present (Fig. 8a). In non-demineralized tissue, the entire lamina densa, apart from the specialized area of bulges, was mineralized, and this mineral deposit was continuous with that of enameloid/dentine (Fig. 8b). Furthermore, overlapping and binding of the organic and mineral phases was shown to occur throughout the internal basement membrane. Thus, in one comparative study (Sawada & Inoue, 2003), it was demonstrated that firm association of the tooth-gingiva occurs according to the same mechanism, that is, partial mineralization of the internal basement membrane, in both mammalian and non-mammalian vertebrates.
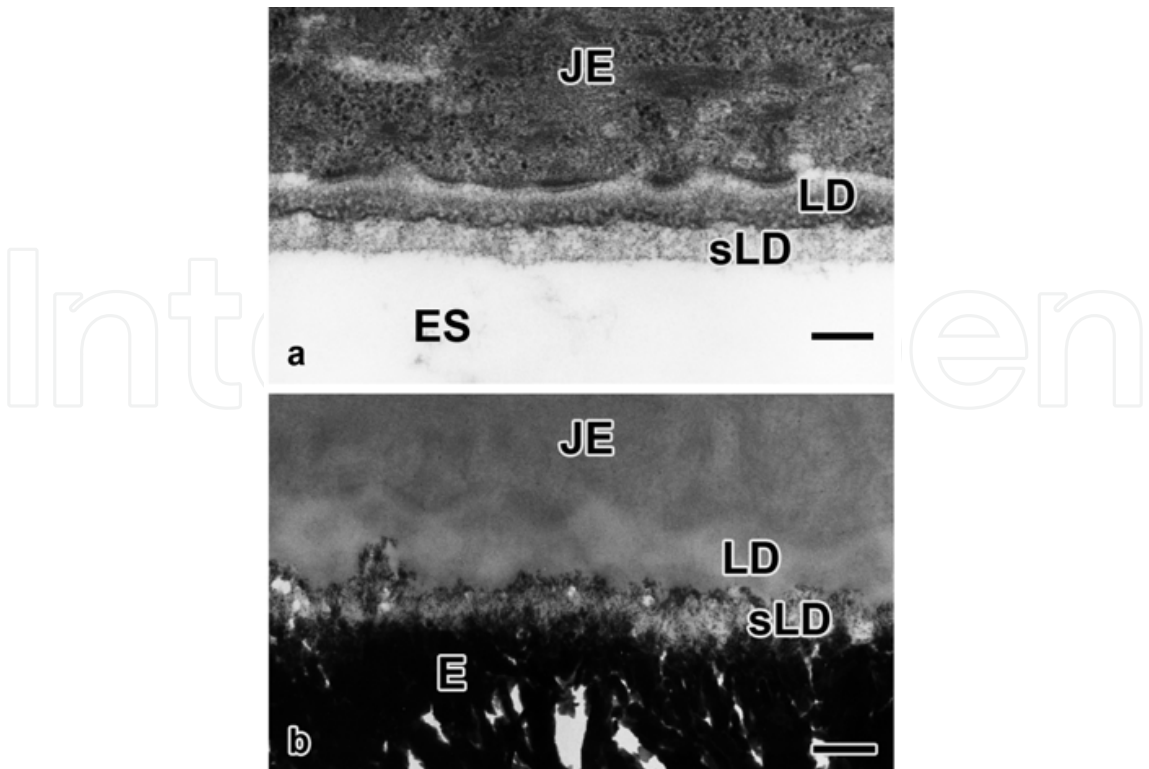
(a) Supplementary lamina densa (sLD) is well preserved after tissue demineralization with EDTA. It is composed of a network of cords similar to that of the internal basement membrane lamina densa (LD). (b) Supplementary lamina densa (sLD) is mineralized with deposit of fine mineral crystals which is continuous with mineral deposited in enamel (E). JE, junctional epithelium; ES, enamel space; LD, lamina densa. Scale bars = 0.2 μm. Modified from Sawada & Inoue, 2003 © Calcified Tissue International.

Fig. 6. Dentogingival border of monkey tooth from demineralized (a) and non-demineralized samples (b)
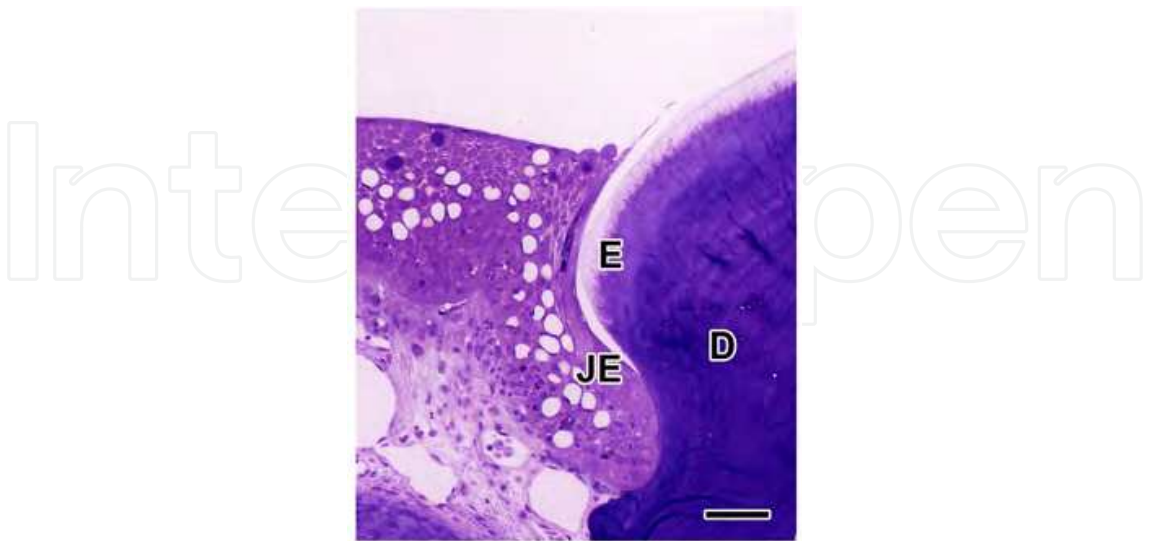
JE, junctional epithelium; E, enameloid; D, dentin. Scale bar = 100 μm. Modified from Sawada & Inoue, 2003 © Calcified Tissue International.

Fig. 7. Light micrograph of area of dentogingival border in shark tooth
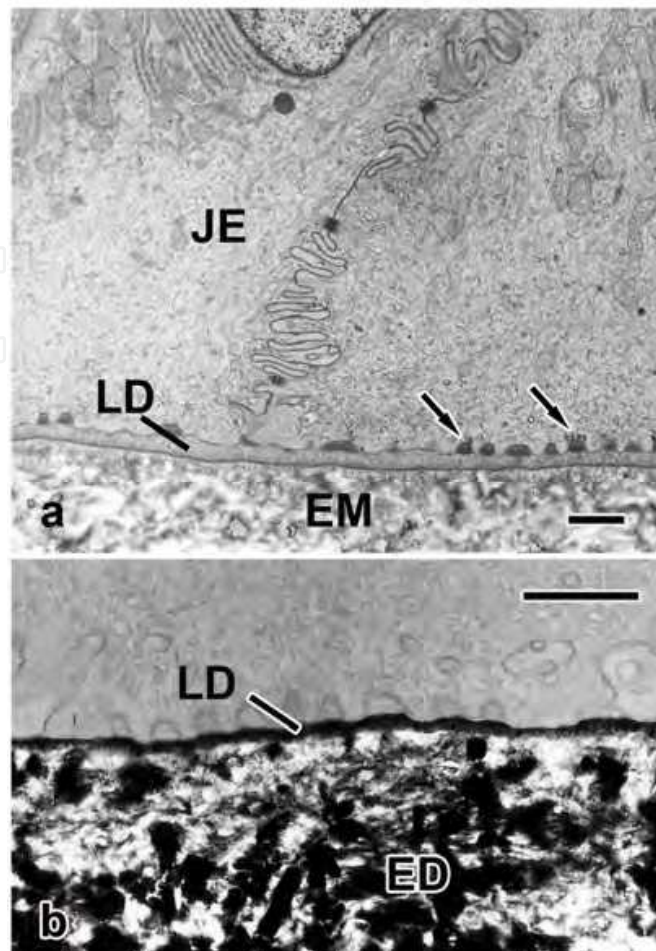
(a) Internal basement membrane of junctional epithelium (JE) is composed of lamina densa (LD) with extremely narrow lamina lucida to which semicircular or rectangular structures (arrows) are associated on its epithelial side. (b) Internal basement membrane at dentogingival border in shark tooth (non-demineralized sample). Lamina densa (LD) of internal basement membrane is mineralized by deposition of fine mineral crystals whose orientation is distinct from that of enameloid (ED). EM, matrix of enameloid/dentin. Scale bars = 1 μm. Modified from Sawada & Inoue, 2003 © Calcified Tissue International.

Fig. 8. Electron micrograph of dentogingival border in cervical region of shark tooth

Similarly, in the maturation stage of amelogenesis in monkey (Sawada & Inoue, 2000), mineralization of the lamina densa-like layer and part of the lamina densa was reported to proceed along the cords, ensuring firm attachment of the organic and mineral phases. The basement membrane of a layer of maturation-stage ameloblasts was specialized, showing an association between the lamina densa at its enamel side and a wider layer of what appeared to be an additional lamina densa (Fig. 9a). Observation of non-demineralized tissue revealed that almost the entire layer of combined lamina densa and its closely associated lamina densa-like structure were associated with enamel crystals, forming with advance in mineralization (Fig. 9b). Again, these grain-like crystals, unlike the larger needle-like crystals of enamel, were arranged along the individual cords of the cord network of the lamina densa or lamina densa-like layer (Sawada & Inoue, 2000).
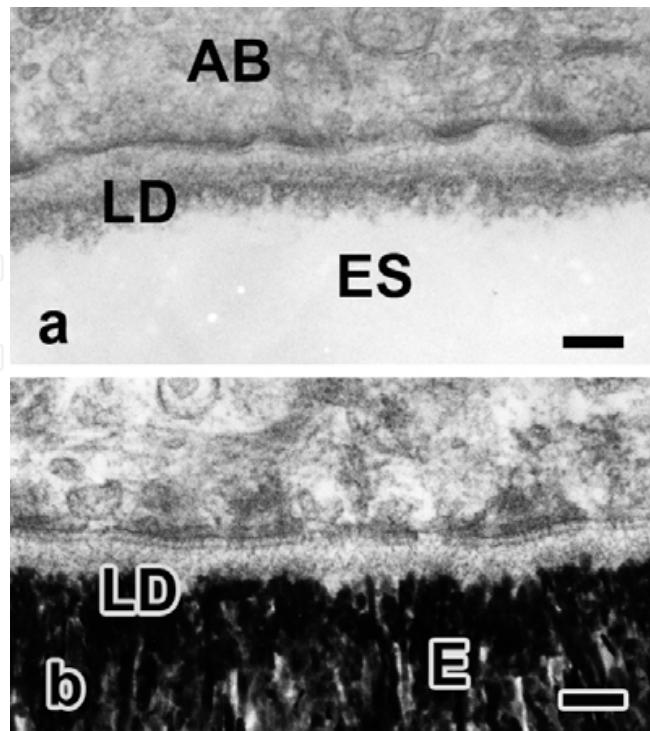
(a) Lamina densa (LD) is composed of cord network. (b) Part of lamina densa (LD) is mineralized and embedded in advancing edge of enamel (E). AB, maturation stage ameloblasts; ES, enamel space. Scale bars = 0.1 μm. Modified from Sawada & Inoue, 2000 © Calcified Tissue International.

Fig. 9. Electron micrograph of basement membrane of maturation stage ameloblasts

3.4 Dentogingival border of replanted tooth

The technique of tooth replantation has successfully been used in endodontic therapy. The original attachment apparatus is likely to be mechanically disrupted immediately following surgery. Regeneration of the attachment apparatus after gingival surgery has been reported (Listgarten, 1967; Maríková, 1983; Masaoka et al., 2009; Taylor & Campbell, 1972). However, whether or not regeneration of the attachment apparatus at the dentogingival border occurs following tooth replantation remains to be clarified. It is known that when replantation of avulsed teeth is delayed, conditions such as desiccation, bacterial infection and added inflammation cause damage to the periodontal ligament and may lead to unfavorable prognoses such as ankylosis. However, if avulsed teeth are immediately replanted with minimum extra-oral dry time, "favorable healing" results, with repair of damaged root surface by cementum (Andreasen, 1981; Line et al., 1974).

In a recent study, tissues around replanted teeth in rat were examined morphologically and ultrastructurally in detail in order to determine whether the attachment apparatus at the dentogingival border was regenerated following replantation (Shioya et al., 2009). Rat molars, luxated and extracted with care to keep damage to the surrounding tissues to a minimum, were immediately replanted into their original sockets. Most of the junctional epithelium at the dentogingival border was lost in one week. The coronal side of the enamel was covered with oral sulcular epithelium, from the tip of which a thin layer of epithelium

formed and extended towards the apical side along the surface of the enamel. At the ultrastructural level, the cells composing this new epithelium closely resembled those of junctional epithelium. In addition, a basement membrane-like layer appeared along the surface of this new epithelium. Although many inflammatory cells were observed invading this area, two weeks later they had disappeared, and at this stage numerous hemidesmosomes appeared on the enamel side of the new epithelium closely attached to a newly formed internal basement membrane (Fig. 10a). Four weeks after replantation, the cells of the newly formed epithelium, which covered the enamel and extended towards the apical side, appeared almost identical to those of the junctional epithelium (Fig. 10b). No inflammation was present in the lamina propria at this stage.
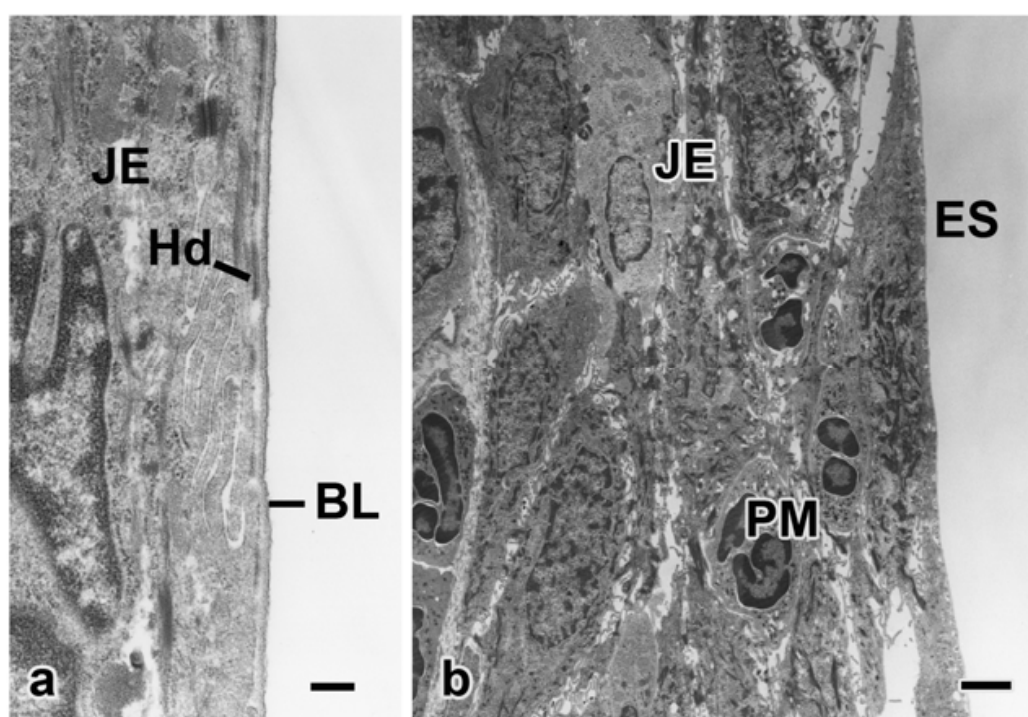
(a) Note occurrence of basal lamina-like structure (BL) at enamel surface. Well differentiated hemidesmosomes (Hd) are evident in regenerated junctional epithelium (JE). (b) Cells of regenerated junctional epithelium (JE) 4 weeks after replantation. Epithelial cells covering enamel were morphologically almost identical to cells of junctional epithelium in control animals. Polymorphonuclear leukocytes (PM) were observed between epithelial cells. ES, enamel space. Scale bars = 0.2 μm (a), 2 μm (b). Modified from Shioya et al., 2009 © Clinical Oral Implants Research.

Fig. 10. Electron micrograph showing interface at 2 (a) and 4 (b) weeks after replantation in rat

3.5 Tissues surrounding dental implants

In addition to tooth replantation, the technique of replacing teeth with dental implants has also been successfully applied (Weber & Fiorellini, 1992). As in tooth replantation, the original attachment apparatus is broken down following surgery. Views in the literature regarding the subsequent regeneration of the attachment apparatus in the peri-implant

epithelium remain conflicting. The aim of the final part of this section is to describe the ultrastructure of the dentogingival border of the dental implant in detail.

3.5.1 Interface between dental implant and epithelium

A number of authors observed eventual restoration of the junctional epithelium at the surface of implants using light microscopy (Abrahamsson et al., 1996, 1999, 2002; Berglundh et al., 1991, 2007; Fujii et al., 1998; Moon et al., 1999; Schüpbach et al., 1994). A few reports dealt with the *in vivo* reconstruction of the attachment apparatus at the electron microscopic level (Gould et al., 1984; Hashimoto et al., 1989; McKinney et al., 1985). Hashimoto et al. (1989) demonstrated that the innermost cells of the peri-implant epithelium in monkey gingiva attached to a single-crystal sapphire dental implant surface by means of basal lamina-like structures and hemidesmosomes at 3 months after implant insertion. In addition, they showed a lack of attachment apparatus at the apical portion of the peri-implant epithelium.

On the other hand, no attachment apparatus was formed between plasma-sprayed ITI implants and the peri-implant epithelium of dogs, and the nature of the epithelium was closer to that of oral mucosal epithelium than to that of junctional epithelium, based on immunohistochemical results (Fujiseki et al., 2003). In their electron micrograph, many microvilli were evident at the periphery of the cells at the implant sites in place of hemidesmosomes and basal lamina after 6 months implantation. In another recent group research, formation of both internal basement membrane and hemidesmosomes was observed only in the lower region of the boundary (Ikeda et al., 2000). The presence of laminin 5, known to be important in epithelial cell adhesion and reported to be localized in the basement membrane of the junctional epithelium in normal tooth (Hormina et al., 1998; Oksanen et al., 2001), was observed by immunoelectron microscopy in the cells of the innermost layer and basal layer of peri-impant mucosa (Atsuta et al., 2005). Internal basement membrane, which also contained laminin 5 and hemidesmosomes, formed an adhesive structure at the apical portion of the interface between implant and peri-implant epithelium (Atsuta et al., 2005). These observations indicate the importance of laminin 5 in the attachment of an implant to the peri-implant epithelium. This notion may be supported by a recent study showing that a laminin-5-derived peptide coating strongly favored *in vitro* formation of adhesion structures (Werner et al., 2009).

We have demonstrated that peri-implant (pure-titanium) epithelium was formed at 1 week after implantation in rat. At 8 weeks after implantation, the leading edge of the peri-implant epithelium receded in the direction of the gingival crest, and this epithelium showed the characteristics of oral sulcular epithelium at the light microscopic level (Fig. 11a). In detailed examination, we showed that binding of the pure-titanium implant and the peri-implant epithelium was imperfect at the ultrastructural level. That is, neither hemidesmosomes nor basal lamina were present at the interface between the epithelium and the implant (Fig. 11b). No cells with the morphology of junctional epithelium were observed in the peri-implant epithelium, unlike with tooth replantation.

The discrepancies between these results were probably caused by a number of factors, including implant diameter, contact surface topology, surgical protocol, experimental period, and animal model used. A preliminary animal experiment was performed to determine whether regeneration of the attachment apparatus was influenced when $CaTiO_3$ implants were replaced with pure-titanium implants.
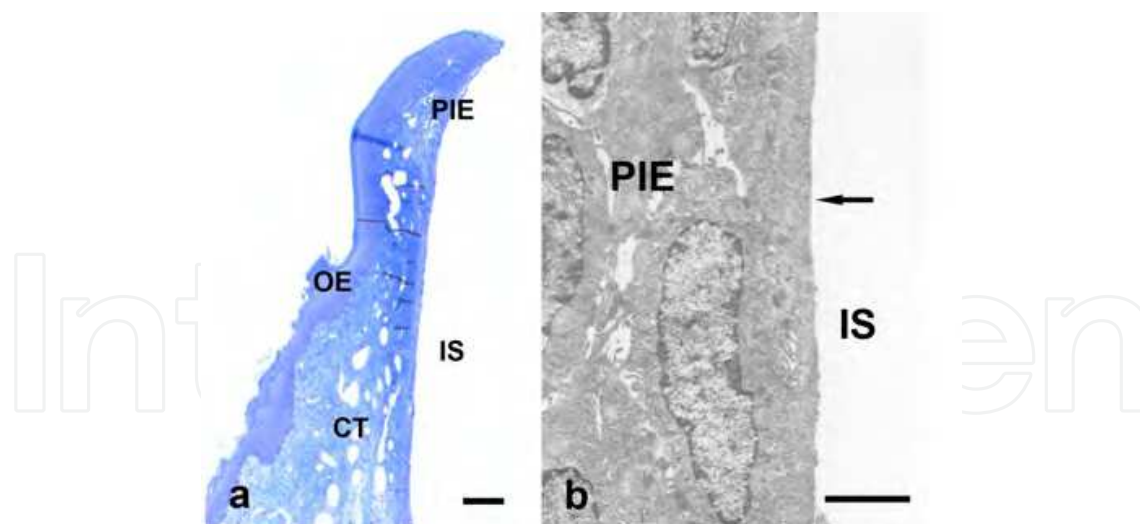
(a) Coronal side of pure titanium implant was covered by peri-implant epithelium (PIE). (b) Peri-implant epithelial-cells (PIE) resembled oral sulcular epithelial cells of control rat. Note no attachment apparatus at implant surface (arrow). CT, connective tissue; IS, implant space; OE, oral epithelium. Scale bars = 100 μm (a), 2 μm (b). Modified from Shioya et al., 2009 © Clinical Oral Implants Research.

Fig. 11. Light micrograph (a) and electron micrograph (b) of peri-implant epithelium

The results showed that no attachment apparatus was organized between the peri-implant epithelium and the $CaTiO_3$ implant (Fig. 12: unpublished data). This suggests that the surface topography of an implant does not, at least, influence the regeneration of the basal lamina or hemidesmosomes at the interface between the dental implant and the epithelium. Attachment of soft tissue to titanium implants was found not to be influenced by the roughness of the surface of the implant (Abrahamsson et al, 2002). These findings are consistent with a recent report by de Sanctis et al. (2009) showing that different implant designs and implant surfaces did not significantly influence bone healing at fresh extraction sockets.
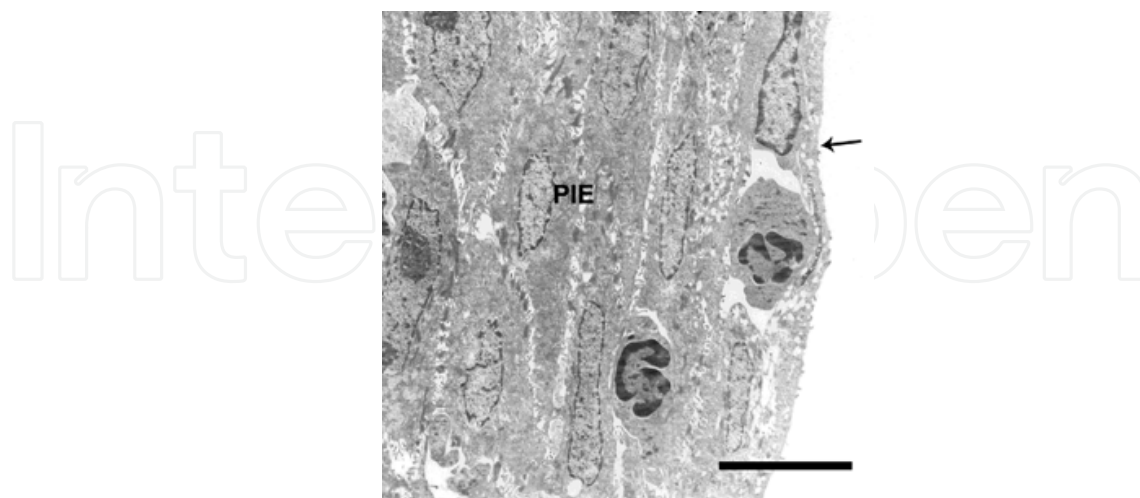
Peri-implant epithelium (PIE) lacked attachment apparatus at interface with implant surface (arrow). Scale bar = 5 μm.

Fig. 12. Electron micrograph of peri-implant epithelium at 8 weeks after implantation ($CaTiO_3$ implant)

3.5.2 Interface between dental implant and connective tissue

Alternative structures of peri-implant tissues were reported (Abrahamsson et al., 2002; Berglundh et al., 2007; Moon et al., 1999; Shioya et al., 2009). A layer of aligned, epithelial-like cells emerged within peri-implant tissue, and this cell layer was unaccompanied by any structures related to attachment apparatus, including hemidesmosomes or basement membrane (Fig. 13). This cell layer was surrounded by bundles of collagen fibrils and elongated fibroblasts oriented parallel to the long axis of the implant. This structure was thought to seal the peri-implant tissue from the oral environment. The biological significance of the epithelium-like layer of cells is not clear, but it may, as Abrahamsson et al. (2002) suggested, cooperate with fibroblasts to help stabilize peri-implant tissues.

In a very recent study, Rinaldi & Arana-Chavez (2010) investigated the ultrastructure of the interface between periodontal tissues and orthodontic titanium mini-implants in rat mandibles. The results demonstrated that a thin cementum-like layer was formed at longer times after implantation at the interface between the surface of the implant and the periodontal ligament. The cementum-like layer contained some collagen fibrils, although it did not contain collagen fiber bundles such as Sharpey's fibers from the periodontal ligament.

Therefore, the next step of our study is to elucidate the origin of epithelial-like cells and their possible functional role in the formation of the cementum-like structure forming at the interface with the implant surface.
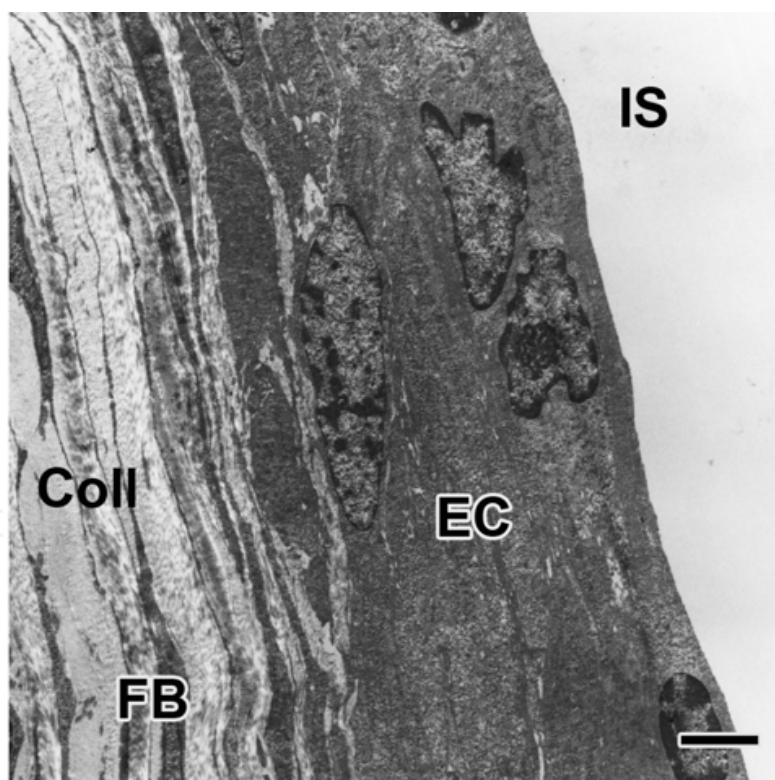
Cells (EC) showing epithelial-like alignment with narrow intercellular spaces were observed in peri-implant connective tissue, which was closely attached to implant. Cells had numerous ribosomes and a large amount of rough endoplasmic reticulum. Fibroblasts (FB) among bundles of collagen fibers (Coll) were oriented parallel to long axis of implant. IS, implant space. Scale bar = 2 μm. Modified from Shioya et al., 2009 © Clinical Oral Implants Research.

Fig. 13. Interface of peri-implant connective tissue 8 weeks after implantation

4. Conclusion

The internal basement membrane of the junctional epithelium at the dentogingival border in normal tooth is specialized for mechanical strength by means of its much wider lamina densa with unusually thick cords. In addition, strong gingival-tooth adhesion is established by partial mineralization of the internal basement membrane.

Newly formed internal basement membrane and numerous hemidesmosomes were observed between regenerated junctional epithelium and replanted teeth. On the other hand, peri-implant epithelium was preserved in the form of oral sulcular epithelium, and neither junctional epithelium nor attachment apparatus was restored after implantation. An alternative structure in peri-implant tissues was observed, comprising a layer of aligned, epithelial-like cells surrounded by collagen fiber bundles. The role of this epithelium-like layer may be stabilization of peri-implant tissues together with fibroblasts.

5. Acknowledgment

6. References

Abrahamsson, I., Berglundh, T., Wennström, J., & Lindhe, J. (1996). The peri-implant hard and soft tissues at different implant systems. A comparative study in the dog. *Clin Oral Implants Res*, 7(3):212-219.

Abrahamsson, I., Berglundh, T., Moon, I.S., & Lindhe, J. (1999). Peri-implant tissues at submerged and non-submerged titanium implants. *J Clin Periodontol*, 26(9):600-607.

Abrahamsson, I., Zitzmann, N.U., Berglundh, T., Linder, E., Wennerberg, A., & Lindhe, J. (2002). The mucosal attachment to titanium implants with different surface characteristics: an experimental study in dogs. *J Clin Periodontol*, 29(5):448-455.

Andreasen, J.O. (1981). Relationship between cell damage in the periodontal ligament after replantation and subsequent development of root resorption. A time-related study in monkeys. *Acta Odontol Scand*, 39(1):15-25.

Atsuta, I., Yamaza, T., Yoshinari, M., Goto, T., Kido, M.A., Kagiya, T., Mino, S., Shimono, M., & Tanaka, T. (2005). Ultrastructural localization of laminin-5 (γ 2 chain) in the rat peri-implant oral mucosa around a titanium-dental implant by immuno-electron microscopy. *Biomaterials*, 26(32):6280-6287.

Berglundh, T., Lindhe, J., Ericsson, I., Marinello, C.P., Liljenberg, B., & Thomsen, P. (1991). The soft tissue barrier at implants and teeth. *Clin Oral Implants Res*, 2(2):81-90.

Berglundh, T., Abrahamsson, I., Welander, M., Lang, N.P., & Lindhe, J. (2007). Morphogenesis of the peri-implant mucosa: an experimental studt in dogs. *Clin Oral Implants Res*, 18(3):1-8.

Bosshardt, D.D. & Lang, N.P. (2005). The junctional epithelium: from health to disease. *J Dent Res*, 84(1): 9-20.

de Sanctis, M., Vignoletti, F., Discepoli, N., Zucchelli, G., & Sanz, M. (2009). Immediate implants at fresh extraction sokets: bone healing in four different implant systems. *J Clin Periodontol*, 36(8)705-711.

Eady, R.A. (1994). The hemidesmosome: a target in auto-immune bullous disease, *Dermatology*, 189(Suppl 1):38-41.

Eide, B., Lie, T., & Selvig, K.A. (1983). Surface coatings on dental cementum incident to periodontal disease. I. A scanning electron microscopic study. *J Clin Periodontol*, 10(2):157-171.

Frank, R.M. & Cimasoni, G. (1970). Ultrastructure de l epithelium cliniquement normal du sillon et la junction gingivo-dentaires. *Z Zellforsch Mikrosk Anat*, 109(3):356-379.

Friedman, M.T., Barber, P., & Newman, H.N. (1993). Ultrastructure and histochemistry of the dental cuticle in adult periodontitis. *J Periodontol*, 64(6):520-528.

Fujii, N., Kusakari, H., & Maeda, T. (1998). A histological study on tissue responses to titanium implantation in rat maxilla: the process of epithelial regeneration and bone reaction. *J Periodontol*, 69(4): 485-495.

Fujiseki, M., Matsuzaka, K., Yoshinari, M., Shimono, M., & Inoue, T. (2003). An experimental study on the features of peri-implant epithelium: immunohistochemical and electron-microscopic observations. *Bull Tokyo Dent Coll*, 44(4):185-199.

Garrod, D.R. (1993). Desmosomes and hemidesmosomes. *Curr Opin Cell Biol*, 5(1):30-40.

Gould, T.R.L., Westbury, L., & Brunette, D.M. (1984). Ultrastructural study of the attachment of human gingiva to titanium in vivo. *J Prosthet Dent*, 52(3):418-420.

Hashimoto, M., Akagawa, Y., Nikai, H., & Tsuru, H. (1989). Ultrastructure of the peri-implant junctional epithelium on single-crystal sapphire endosseous dental implant loaded with functional stress. *J Oral Rehabil*, 16(3):261-270.

Hodson, J.J. (1966). A critical review of the dental cuticle with special reference to recent investigations. *Int Dent J*, 16(3):350-384.

Hormina, M., Sahlberg, C., Thesleff, I., & Airenne, T. (1998). The epithelium-tooth interface - a basal lamina rich in laminin-5 and lacking other known laminin isoforms. *J Dent Res*, 77(7):1479-1485.

Ihara, I., Miake, Y., Morinaga, K., Yatsuhashi, T., Nakagawa, K., & Yanagisawa, T. (2007). Calcification of pulp canal space after replantation of immature rat molars. *J Hard Tissue Biol*, 16(2):54-60.

Ikeda, H., Yamaza, T., Yoshinari, M., Ohsaki, Y., Ayukawa, Y., Kido, M.A., Inoue, T., Shimono, M., Koyano, K., & Tanaka, T. (2000). Ultrastructural and immunoelectron microscopic studies of the peri-implant epithelium-implant (Ti-6Al-4V) interface of rat maxilla. *J Periodontol*, 71(6): 961-973.

Inoue, S. (1989). Ultrastructure of basement membranes. *Int Rev Cytol*, 117:57-98.

Inoue, S. (1994). Basic structure of basement membranes is a fine network of "cords," irregular anastomosing strands. *Microsc Res Tech*, 28(1):29-47.

Inoue, S. & Leblond, C.P. (1988). Three-dimensional network of cords: The main component of basement membranes. *Am J Anat*, 181(4):341-358.

Inoué, S., Leblond, C.P., & Laurie, G.W. (1983). Ultrastructure of Reichert's membrane, a multilayered basement membrane in the parietal wall of the rat yolk sac. *J Cell Biol,* 97(5 Pt 1), 1524-1537.

Ito, H., Enomoto, S., & Kobayashi, K. (1967). Electron microscopic study of the human epithelial attachment. *Bull Tokyo Med Dent Univ*, 14(2): 267-277.

Jollie, W.P. (1968). Changes in the fine structure of the parietal yolk sac of the rat placenta with increasing gestational age. *Am J Anat*, 122(3):513-531.

Kobayashi, K. & Rose, G.G. (1978). Ultrastructural histochemistry of the dento-epithelial junction. II. Colloidal thorium and ruthenium red. *J Periodontal Res*, 13(2):164-172.

Kobayashi, K. & Rose, G.G. (1979). Ultrastructural histochemistry of the dento-epithelial junction. 3. Chloramine T-silver methenamine. *J Periodontal Res*, 14(2):123-131.

Kobayashi, K., Rose, G.G., & Mahan, C.J. (1976). Ultrastructure of the dento-epithelial junction. *J Periodontal Res*, 11(6):313-330.

Lie, T. & Selvig, K.A. (1975). Formation of an experimental dental cuticle. *Scand J Dent Res*, 83(3):145-152.

Line, S.E., Polson, A.M., & Zander, H.A. (1974). Relationship between periodontal injury, selective cell repopulation and ankylosis. *J Periodontol,* 45(10):725-730.

Listgarten, M.A. (1966). Electron microscopic study of the gingivo-dental junction of man. *Am J Anat*, 119(1):147-177.

Listgarten, M.A. (1967). Electron microscopic features of the newly formed epithelial attachment after gingival surgery. A preliminary report. *J Periodontal Res*, 2(1):46-52.

Listgarten, M.A. (1970). Changing concepts about the dento-epithelial junction. *J Can Dent Assoc*, 36(2): 70-75.

Listgarten, M.A. (1972). Electron microscopic study of the junction between surgically denuded root surfaces and regenerated periodontal tissues. *J Periodontal Res*, 7(1):68-90.

López, N.J., Gigoux, C., & Canales, M.L. (1990). Morphologic and histochemical characteristics of the dental cuticle in teeth affected by prepubertal periodontitis. *J Periodontol*, 61(2): 95-102.

Maríková, Z. (1983). Ultrastructure of normal and newly formed dento-epithelial junction in rats. *J Periodontal Res*, 18(5):459-468.

Marks, S.C.Jr., McKee, M.D., Zalzal, S., & Nanci, A. (1994). The epithelial attachment and the dental junctional epithelium: ultrastructural features in porcine molars. *Anat Rec*, 238(1):1-14.

Masaoka, T., Hashimoto, S., Kinumatsu, T., Jung, H.S., Yamada, S., & Shimono, M. (2009). Immunolocalization of laminin and integrin in regenerating junctional epithelium of mice after gingivectomy. *J Periodontal Res*, 44(4):489-495.

Matsson, L., Theilade, J., & Attström, R. (1979). Electron microscopic study of junctional and oral gingival epithelia in the juvenile and adult beagle dog. *J Clin Periodontol*, 6(6):425-436.

McKinney, R.V. Jr., Steflik, D.E., & Koth, D.L. (1985). Evidence for a junctional epithelial attachment to ceramic dental implants. A transmission electron microscopic study. *J Periodontol*, 56(10): 579-591.

Moon, I.S., Berglundh, T., Abrahamsson, I., Linder, E., & Lindhe, J. (1999). The barrier between the keratinized mucosa and the dental implant. An experimental study in the dog. *J Clin Periodontol*, 26(10): 658-663.

Nagatsuka, M. (1983). Ultrastructure of the odonto-gingival junction of Japanese monkey (*Macaca fuscata*). *Shikwa Gakuho* 83(11):1387-1435.

Oksanen, J., Sorokin, L.M., Virtanen, I., & Hormina, M. (2001). The junctional epithelium around murine teeth differs from gingival epithelium in its basement membrane composition. *J Dent Res*, 80(12): 2093-2097.

Rinaldi, J.C. & Arana-Chavez, V.E. (2010). Ultrastructure of the interface between periodontal tissues and titanium mini-implants. *Angle Orthod*, 80(3):459-465.

Sato, T. (1973). An electron microscopic observation on epithelial attachment. Epithelial attachment of early stage of inflammed gingiva. *J Jpn Soc Periodontol*, 15(1):3-28.

Sawada, T. & Inoue, S. (1996). Ultrastructural characterization of internal basement membrane of junctional epithelium at dentogingival border. *Anat Rec*, 246(3), 317-324.

Sawada, T. & Inoue, S. (2000). Specialized basement membrane of monkey maturation stage ameloblasts mediates firm ameloblast-enamel association by its partial calcification. *Calcif Tissue Int*, 66(4), 277-281.

Sawada, T. & Inoue, S. (2001a). Ultrastructure and composition of basement membranes in the tooth. *Int Rev Cytol*, 207,151-194.

Sawada, T. & Inoue, S. (2001b). High resolution ultrastructural reevaluation of dental cuticle in monkey tooth. *J Periodontal Res*, 36(2):101-107.

Sawada, T. & Inoue, S. (2003). Mineralization of basement membrane mediates dentogingival adhesion in mammalian and nonmammalian vertebrates. *Calcif Tissue Int*, 73(2):186-195.

Schroeder, H.E. (1969). Ultrastructure of the junctional epithelium of the human gingiva. *Helv Odontol Acta*, 13(2), 65-83.

Schroeder, H.E. (1986). The periodontium, *in* A.Oksche & L. Vollrath (eds.), *Handbook of Microscopic Anatomy,*Vol. v/5., Springer-Verlag, Berlin, pp. 233-313.

Schroeder, H.E. & Listgarten, M.A. (1971). Fine structure of the developing epithelial attachment of human teeth, *in* A. Wolsky (ed.), *Monographs in developmental biology*, Vol. 2, Karger, Basel, pp. 1-134.

Schroeder, H.E. & Listgarten, M.A. (1977). Fine structure of the developing epithelial attachment of human teeth, *in* A. Wolsky (ed.), *Monographs in Developmental Biology*, Vol. 2, 2nd ed., Karger, Basel, pp. 1-136.

Schüpbach, P., Hürzeler, M., & Grunder, U. (1994). Implant-tissue interfaces following treatment of peri-implantitis using guided tissue regeneration: a light and electron microscopic study. *Clin Oral Implants Res*, 5(2):55-65.

Shioya, K., Sawada, T., Miake, Y., Inoue, S., & Yanagisawa, T. (2009). Ultrastructural study of tissues surrounding replanted teeth and dental implants. *Clin Oral Implants Res*, 20(3):299-305.

Stern, I.B. (1981). Current concepts of the dentogingival junction: the epithelial and connective tissue attachments to the tooth. *J Periodontol*, 52(9):465-476.

Taylor, A.C. & Campbell, M.M. (1972). Reattachment of gingival epithelium to the tooth. *J Periodontol*, 43(5):281-293.

Weber, H.P. & Fiorellini, J.P. (1992). The biology and morphology of the implant-tissue interface, *Alpha Omegan*, 85(4):61-64.

Werner, S., Huck, O., Frisch, B., Vautier, D., Elkaim, R., Voegel, J.C., Brunel, G., & Tenenbaum, H. (2009). The effect of microstructured surfaces and laminin-derived peptide coatings on soft tissue interactions with titanium dental implants. *Biomaterials*, 30(12):2291-2301.
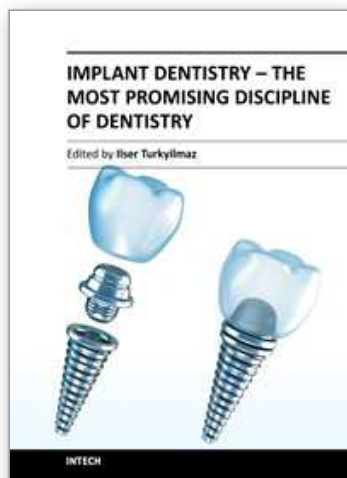
Implant Dentistry - The Most Promising Discipline of Dentistry

Edited by Prof. Ilser Turkyilmaz

ISBN 978-953-307-481-8

Hard cover, 476 pages

Publisher InTech

Published online 30, September, 2011

Published in print edition September, 2011

Since Dr. Branemark presented the osseointegration concept with dental implants, implant dentistry has changed and improved dramatically. The use of dental implants has skyrocketed in the past thirty years. As the benefits of therapy became apparent, implant treatment earned a widespread acceptance. The need for dental implants has resulted in a rapid expansion of the market worldwide. To date, general dentists and a variety of specialists offer implants as a solution to partial and complete edentulism. Implant dentistry continues to advance with the development of new surgical and prosthodontic techniques. The purpose of Implant Dentistry - The Most Promising Discipline of Dentistry is to present a comtemporary resource for dentists who want to replace missing teeth with dental implants. It is a text that integrates common threads among basic science, clinical experience and future concepts. This book consists of twenty-one chapters divided into four sections.

How to reference

In order to correctly reference this scholarly work, feel free to copy and paste the following:

Takashi Sawada and Sadayuki Inoue (2011). Ultrastructure of Dentogingival Border of Normal and Replanted Tooth and Dental Implant, Implant Dentistry - The Most Promising Discipline of Dentistry, Prof. Ilser Turkyilmaz (Ed.), ISBN: 978-953-307-481-8, InTech, Available from: http://www.intechopen.com/books/implant-dentistry-the-most-promising-discipline-of-dentistry/ultrastructure-of-dentogingival-border-of-normal-and-replanted-tooth-and-dental-implant

INTECH
open science | open minds